The *pam1* Gene Is Required for Meiotic Bouquet Formation and Efficient Homologous Synapsis in Maize (*Zea mays* L.)

Inna N. Golubovskaya,* Lisa C. Harper,† Wojciech P. Pawlowski,† Denise Schichnes‡ and W. Zacheus Cande*,†,[1]

**Department of Plant and Microbial Biology, †Department of Molecular and Cell Biology and ‡CNR Biological Imaging, University of California, Berkeley, California 94720-3200*

Manuscript received June 14, 2002
Accepted for publication September 25, 2002

ABSTRACT

The clustering of telomeres on the nuclear envelope (NE) during meiotic prophase to form the bouquet arrangement of chromosomes may facilitate homologous chromosome synapsis. The *pam1* (***p****lural* ***a****bnormalities of* ***m****eiosis* ***1***) gene is the first maize gene that appears to be required for telomere clustering, and homologous synapsis is impaired in *pam1*. Telomere clustering on the NE is arrested or delayed at an intermediate stage in *pam1*. Telomeres associate with the NE during the leptotene-zygotene transition but cluster slowly if at all as meiosis proceeds. Intermediate stages in telomere clustering including miniclusters are observed in *pam1* but not in wild-type meiocytes. The tight bouquet normally seen at zygotene is a rare event. In contrast, the polarization of centromeres *vs.* telomeres in the nucleus at the leptotene-zygotene transition is the same in mutant and wild-type cells. Defects in homologous chromosome synapsis include incomplete synapsis, nonhomologous synapsis, and unresolved interlocks. However, the number of RAD51 foci on chromosomes in *pam1* is similar to that of wild type. We suggest that the defects in homologous synapsis and the retardation of prophase I arise from the irregularity of telomere clustering and propose that *pam1* is involved in the control of bouquet formation and downstream meiotic prophase I events.

MEIOSIS is a specialized cell division producing four daughter cells, each containing a haploid genome complement. Its mechanism is highly conserved throughout eukaryotes (John 1990). One of the least understood processes of meiotic prophase I is the mechanism of homologous chromosome alignment (pairing) and the subsequent formation of the synaptonemal complex between them (synapsis). In the majority of organisms studied, homologous chromosome pairing is immediately preceded in early zygotene by a profound chromosome reorganization, the clustering of telomeres to form the bouquet (reviewed in Dernburg *et al.* 1995; Zickler and Kleckner 1998). It has been assumed that the bouquet facilitates homolog interactions (Loidl 1990; Scherthan 2001 for review). As the telomeres cluster, the ends of all chromosomes come into close proximity and become codirectional, reducing the volume and complexity of the homology search. The evolutionary conservation of the bouquet among fungi, plants, and animals (reviewed by Dernburg *et al.* 1995) and its temporal appearance coincident with the initiation of homolog pairing (Bass *et al.* 2000) suggest it is somehow important in mediating the homology search.

The bouquet is thought to form in two steps: first, telomeres attach to the inner surface of the nuclear envelope and, second, they coalesce into a tight cluster (Gelei 1921; von Wettstein *et al.* 1984; Bass *et al.* 2000; Scherthan *et al.* 2000). In maize, the telomere bouquet arises *de novo*. It has been shown that the Rabl configuration, in which centromeres and telomeres occupy opposite sides of the nucleus due to the previous mitotic anaphase, does not influence the creation of the bouquet (Bass *et al.* 1997; Dong and Jiang 1998; Cowan *et al.* 2001; Carlton and Cande 2002). Further, chromosome ends are not required for entry into the bouquet because ring chromosomes containing telomere sequences enter the bouquet (Carlton and Cande 2002).

Only a handful of genes have been shown to be directly involved in the control of bouquet formation; *taz1* and *lot2-s17/rap1* in fission yeast and *ndj1/tam1* in budding yeast are the most well studied (Cooper *et al.* 1997; Nimmo *et al.* 1998; Trelles-Sticken *et al.* 2000). In the absence of TAZ1, a telomere-binding protein that modulates telomere repeat copy number, telomere clustering is disrupted, there is improper chromosome alignment, and meiotic recombination is significantly decreased (Cooper *et al.* 1998; Nimmo *et al.* 1998). The NDJ1 telomeric protein is absolutely required for bouquet formation in budding yeast and appears to be necessary for proper homologous synapsis, formation of crossovers, and segregation of homologs. In addition, *ndj1* displays a considerable delay in meiotic prophase

[1]*Corresponding author:* University of California, Department of Molecular and Cell Biology, 345 Life Science Addition, Berkeley, CA 94720. E-mail: zcande@uclink4.berkeley.edu

(Chua and Roeder 1997; Conrad *et al.* 1997; Trelles-Sticken *et al.* 2000). Five other fission yeast mutants, four defined by ***d**efective **o**rganization of **t**elomeres* (*dot*) and *kms1*, cause improper telomere clustering, a defective or dispersed spindle pole body, and sterility (Shimanuki *et al.* 1997; Jin *et al.* 2002). In rye, the asynaptic mutant *sy1* also fails to form a bouquet (Mikhailova *et al.* 2001). The phenotypes of this collection of mutants show that mutants defective in bouquet formation are also deficient in homologous synapsis; however, mutants deficient in homologous synapsis can have normal bouquets. These observations suggest that homologous chromosome synapsis is an event downstream from bouquet formation.

We have reexamined our collection of mutants to determine whether any of the known maize meiotic mutants that are deficient in homologous chromosome synapsis are also deficient in bouquet formation. In this article we use state-of-the-art microscopy to show that the primary lesion in the maize meiotic mutant *pam1* (***p**lural **a**bnormalities of **m**eiosis **1***) is the clustering of telomeres on the nuclear envelope (NE). On the basis of our analysis, we suggest that the *pam1* gene product is involved in the control of the bouquet formation and subsequent meiotic prophase I events. When the *pam1* mutant was discovered in 1974, it was described as having multiple meiotic defects, including a prominent asynchrony of meiotic prophase. In contrast to wild-type anthers where all meiocytes are at the same stage of development within one anther, the meiocytes in *pam1* anthers were present in many different stages of meiosis, from zygotene to tetrads (Golubovskaya and Mashnenkov 1977). No previously described maize meiotic mutant has this phenotype. Female meiosis in the *pam1* mutant showed a phenotype more severely retarded than that of male meiosis, and a majority of the megaspore mother cells (MMCs, the female meiocytes) are delayed or arrested in prophase I. Some meiocytes proceed as far as diakinesis-metaphase I and these display improper synapsis. Their nuclei contain univalents as well as bivalents at diakinesis and metaphase I. A few MMCs complete meiosis and develop into regular eight-nuclear-embryo sacs, and these can produce a few normal kernels per ear (Golubovskaya *et al.* 1994). While these early studies did characterize the multiple defects in meiotic prophase chromosome behavior in *pam1* mutants, it was not possible to pinpoint the earliest visible mutant phenotype, and thus it has remained hard to understand the role of the wild-type gene product.

In this study we show that the leptotene-zygotene transition is the first stage where irregularities of meiosis occur in *pam1*. Telomere reorganization into a tight bouquet appears to be arrested or delayed at an intermediate stage in *pam1*; although telomeres are attached to the nuclear envelope, they cluster slowly if at all. The frequency of homologous pairing is low in *pam1* meiocytes as monitored by fluorescence *in situ* hybridization (FISH) using the 5S rDNA locus. Many aspects of homologous chromosome synapsis are abnormal in *pam1*, and defects include incomplete synapsis, nonhomologous synapsis, and unresolved interlocks. We show here that the *pam1* gene maps to chromosome 1 of maize and is not allelic to ***as**ynaptic**1*** (*as1*; bin 1.05), which also maps on the same chromosome.

MATERIALS AND METHODS

Plants: The *pam1* mutant is recessive and was originally induced by *N*-nitroso-*N*-methylurea in the A344 inbred in 1974 (Golubovskaya and Mashnenkov 1977). The *pam1* mutants are completely male sterile and almost completely female sterile, but occasionally a few kernels can be obtained from crosses of normal pollen onto *pam1* ears. Families of plants segregating in a 1:1 or 3:1 ratio for fertile plants with normal meiosis and male sterile plants with a cytologically mutant phenotype were used in this study. (Families segregated 3:1 are the progeny of self-pollinated *pam1*/+ heterozygotes. Families segregated 1:1 were produced by crosses of homozygous sterile *pam1* mutants with heterozygous sibs). For FISH, immunostaining, and transmission electron microscopy (TEM), *pam1* mutants maintained in the A344 background were used. For mapping, hybrid plants were used.

as1 is the first reported meiotic mutant in maize and it arose spontaneously. It has abnormalities in chromosome synapsis (Beadle 1930; Maguire and Riess 1991) and is genetically located in bin 1.05 (http://www.agron.missouri.edu/locus.html). The mutant was used in this study only for complementation tests with *pam1*. *as1* mutants are male sterile, but partially female fertile, so they can be used as females in complementation tests. I. Golubovskaya obtained this stock from the Maize Stock Center many years ago.

Genetics: To map the *pam1* gene to a maize chromosome arm, waxy-marked reciprocal translocations were used (Laughnan and Gabay-Laughnan 1994). A total of 10 different waxy translocations were used: wx1-9c (1S.47: 9L.22), wx1-9 (5622) (1L.10: 9L.12), wx1-9 (4995) (1L.19: 9S.20), wx2-9d (2L.83: 9L.27), wx3-9 (8447) (3S.44: 9L.14), wx3-9c (3L.09: 9L.12), wx4-9e (4S.53: 9L.26), wx4-9 (5657) (4L.33: 9S.25), wx5-9 (4817) (5L.06: 9S.07), and wx6-9 (4778) (6S.80: 9 L.30).

Heterozygous *pam1*/+ plants (resulting from a cross of *pam1*/+ fertile pollen onto *pam1*/*pam1* mutant sib ears) were used as male parents to cross onto the ears of this translocation set. F_1 seeds were grown to maturity and self-pollinated. The resulting F_2 progeny were analyzed for segregation for male sterility and waxy. Linkage of *pam1* to the chromosome 1 translocations was determined by segregation analysis, and an estimate of map distance was calculated with the product method for these two genes (*waxy* and *pam1*) in repulsion (Redei 1998).

To test allelism of *pam1* with *as1*, homozygous *as1*/*as1* plants were used as female parents in crosses with heterozygous *pam1*/+. The F_1 progeny were grown in the greenhouse and meiocytes from all individual plants were collected and examined by light microscopy to determine if they exhibited a mutant phenotype. In addition, the F_1 progeny of reciprocal crosses of heterozygous plants of the two mutants were examined for segregation of male sterility in the summer field nursery.

Cytology: A smear acetocarmine technique was routinely used for confirming the *pam1* mutant phenotype in plants from *pam1* families that segregated a male sterile phenotype. Immature tassels were fixed in Farmer's fixative (3:1 ratio of 95% ethanol to glacial acetic acid) and stained with 2%

acetocarmine, squashed, and observed with a light microscope (Golubovskaya *et al.* 1993).

Transmission electron microscopy: A spread technique was used to characterize synapsis of prophase I chromosomes in *pam1/pam1* mutants and wild-type siblings by TEM. A suspension of meiocytes was prepared from fresh anthers containing meiocytes at a known stage of prophase I, as previously identified by examination under the light microscope. The suspension of whole nuclei was spread on the surface of 0.2 M sucrose (S-0389, Sigma, St. Louis) solution, placed on Falcon plastic-coated slides, fixed by exposure to the vapor of a 37% formalin solution (formaldehyde F1635, Sigma) for 1–4 hr, dried for 2–3 days at room temperature, washed in deionized water, dried again, and stained with 50–70% silver nitrate (S-0139, Sigma) according to the protocol of Gillies (Gillies 1981; Golubovskaya *et al.* 1993). A Hitachi 500 microscope was used for the examination of synapsis on spreads of *pam1* prophase I chromosomes. Images were taken on Kodak EM film 4489.

Fixation and preparation of meiocytes for FISH and immunostaining: Anthers from developing tassels were staged with the acetocarmine squash technique. Anthers from the same floret and from those in close proximity and thus close in developmental age were fixed at room temperature in 4 ml of 4% formaldehyde in Buffer A (15 mM Pipes − NaOH, pH 6.8, 80 mM KCl, 20 mM NaCl, 0.5 mM EGTA, 2 mM EDTA, 0.15 mM spermine tetra HCL, 0.05 mM spermidine, 1 mM dithiothreitol, 0.32 M sorbitol; Bass *et al.* 1997) for 45 min in a gently shaking 10-ml petri dish. They were then washed three times, 30 min each in fresh Buffer A and stored at 4° in the buffer and used within 4 weeks. Fixed anthers were cut open at the tip to release the meiocytes into 100–200 μl of Buffer A. Meiocytes (10 μl) suspended in Buffer A were then transferred by micropipette onto a glass coverslip (22 × 22 mm) followed by the immediate addition of 5 μl of activated acrylamide stock. The activation of acrylamide was done by addition of 5 μl of 20% ammonium persulfate and 5 μl of 20% sodium sulfide to 100 μl of a 15% (29:1 acrylamide:bisacrylamide) gel stock in 1× Buffer A. The slides were rocked and rotated for a few seconds until the drops mixed and a second coverslip was placed on top for 45 min and then removed with a razor blade, leaving a thin pad of acrylamide with embedded meiocytes on the slide (Bass *et al.* 1997).

Probes: A 27-bp oligonucleotide, 5′-CCTAAAGTAGTG GATTGGGCATGTTCG-3′, labeled with either Cy5 or FITC, was obtained from Genset (Paris) and was used to detect the CentC sequence that resides near maize centromeres (Ananiev *et al.* 1998). Oligonucleotides complementary to the telomere repeat (5′-{CCCTAAA}$_4$-3′) and labeled with either Cy5 or FITC (Genset) were used to detect maize telomeres (Bass *et al.* 1997). A 5S rDNA probe was made by PCR. Approximately 1–10 ng of a plasmid containing 5S rDNA sequence from maize (Zimmer *et al.* 1988) was added to a standard PCR reaction mix: 2 μl 10× buffer with 15 mM $MgCl_2$ from Perkin Elmer (Norwalk, CT); 2 μl of forward and reverse primers; 2 μl 1 mM dATP, dGTP, dCTP, a mixture of dTTP and dUTP-FITC, or dUTP-Cy5; 2 units Amplitaq (Perkin-Elmer); and water to 20 μl. For each labeling reaction, a 20-μl unlabeled control reaction was performed, and an aliquot of equal molar volume was run side by side with the labeling reaction in a 4% gel. Incorporation of fluorescent label could sometimes be seen on the transilluminator, but empirical determination of probe effectiveness by FISH was required for each batch of probe made.

FISH and indirect immunofluorescence: Newly polymerized acrylamide pads were washed with 1× PBS to remove unpolymerized acrylamide, followed by four equilibration washes with a prehybridization buffer (50% deionized formamide and 2× SSC). Coverslips were placed on a slide and then 50 μl of probe in prehybridization buffer was added. Slides were then sealed under a second coverslip using rubber cement and incubated at 37° for 30–45 min. The slides were denatured on a PCR block at 96° for 6 min followed by overnight incubation at 30°. The slides were then washed for 30 min sequentially with 1× PBS and 1× SSC (three times), 1× PBS and 0.1% Tween-20 (four times), 1× PBS (three times), and 1× TBS (one time). The slides were then stained with 10 μg/ml 4′,6-diamidino-2-phenylindole, dihydrochloride (DAPI) in 1× TBS for 30 min at room temperature. Excess DAPI was removed by washing with 1× TBS (three times) for a total of 30 min. Slides were then mounted in 1,4 diazabicyclo-[2,2,2] octane (DABCO), sealed with clear fingernail polish, and stored at 20°.

The procedure for staining RAD51 foci using the anti-HsRAD51 rDNA antibody was described previously (Franklin *et al.* 1999) and is briefly outlined here. The coverslips with the polyacrylamide pads containing the fixed meiocytes were prepared the same way as for FISH. After twice washing with 1× PBS for 10 min, cells were permeabilized for 45 min in 1× PBS, 1% Triton X-100, and 1 mM EDTA and then blocked for 1 hr in 1× PBS, 3% BSA, 5% normal donkey serum, 1 mM EDTA, and 0.1% Tween 20. Samples were incubated overnight in a humid chamber with 50 μl of a 1:500 dilution of the anti-HsRAD51 antibody, precleared for 30 min at 4° with *Escherichia coli* XL1-Blue acetone powder in blocking buffer. After 24 hr, slides were washed five to eight times, 1 hr for each wash, in 1× PBS, 0.1% Tween 20, and 1 mM EDTA, with continued washing overnight. Slides were incubated overnight in fluorescein isothiocyanate-labeled donkey anti-rabbit fragment at 1 μg/ml in blocking buffer, and the identical washing protocol was followed the next day and night. Slides were stained with 10 μg/ml DAPI for 30 min in PBS followed by two 1-ml washes of 1× PBS, transferred into DABCO, sealed with clear fingernail polish, and stored at 20°.

Three-dimensional deconvolution light microscopy and image generation: Images were acquired on a Delta Vision (Applied Precision) imaging station: an Olympus IX70 inverted microscope with ×100, 1.35 NA oil-immersion lens and a Photometric (Roper Scientific) charge-coupled device. All images were taken with a Z step size of 0.2 μm, saved as 3-D stacks, and subjected to constraint iterative deconvolution. 3-D data analysis and 2-D image creation were performed using the DeltaVision/soft WoRx software package (Applied Precision) on a Silicon Graphics Workstation. 2-D images were converted to TIFF and opened in Photoshop on a Macintosh computer. Photoshop was used to manipulate false colors and to convert colors from RGB to CMYK for printing.

RESULTS

The *pam1* locus is on chromosome 1: To localize the *pam1* gene to a chromosome arm, we used the standard T-wx method. We crossed pollen from *pam1/+* heterozygotes to several ears from each line of a T-*waxy1* translocation series, self-pollinated the F_1 plants, sorted the F_2 progeny seeds by waxy phenotype (waxy *vs.* starchy), and grew them to maturity for scoring. Examination of the F_2 progeny families showed that *pam1* was linked to three chromosome 1 *waxy* translocations. The F_2 progeny of the cross *pam1/+* onto wx1-9c (1S.47: 9L.22) segregated 64 starchy fertile, 25 starchy male sterile, 50 waxy fertile, and 2 waxy sterile (Table 1A). Analysis of the results by product method showed 21.5 cM between

TABLE 1

Mapping the *pam1* gene with T-waxy translocation series

Analyzed combinations of crosses waxy1 T hom × *pam1*/+	No. of analyzed crosses	Waxy kernels			Starchy kernels		
		Fertile	Sterile	Total	Fertile	Sterile	Total
A. 1S							
1S.47:9L.22	2	50	2	52	64	25	89
B. 1L							
1L.10:9L.12	2	72	0	72	67	19	86
1L.19:9S.20	2	68	0	68	66	20	86
Subtotal	4	140	0	140	133	39	172
C. Other tested translocations							
2L.83:9L.27, 3S.44:9L.14 3L.09:9L.12, 4S.53:9L.26 4L.33:9S.25, 5L.06:9S.07 6S.80:9L.30	24	658	135	793	870	188	1058

pam1 and *waxy1* in this line. This indicates that *pam1* is linked to the short arm of chromosome 1 (1S). The F_2 progeny of the cross of the same *pam1*/+ heterozygote onto both wx1-9 (5622) (1L.10: 9L.12) and wx1-9 (4995) (1L.19: 9S.20) translocations segregated 133 starchy fertile, 39 starchy sterile, 140 waxy fertile, and 0 waxy sterile (Table 1B). This indicates a very tight linkage between *pam1* and the *waxy1* genes in these translocation lines, and thus *pam1* is tightly linked to the long arm of chromosome 1 (1L). Both the 1S and 1L mapping data indicate that the *pam1* gene is close to the centromere. Since it is difficult to map a centromere genetically, we cannot distinguish with these data whether *pam1* is on the short or long arm.

The *pam1* gene did not show any linkage to *wx1* on any translocations of chromosomes other than chromosome 1. The fraction of recombination for the pooled data is estimated at 0.493 (Table 1C), indicating independent assortment.

The *pam1* and *as1* genes are not allelic: The *pam1* gene is the second meiotic gene to map to chromosome 1. The first was *asynaptic 1* (*as1*), which also maps to the centromere region of chromosome 1 (bin 1.05). To determine whether these are alleles of the same gene, a complementation test with the two mutants was performed. Pollen from *pam1*/+ plants was crossed to *as1*/*as1* ears, and a total of 64 resulting F_1 plants were fixed, stained with acetocarmine, and examined by light microscopy. All 64 appeared to be fertile with normal meiosis. Moreover, all 76 F_1 plants from reciprocal crosses of *as1*/+ and *pam1*/+ also exhibited a fertile phenotype in field. These results indicate that *pam1* and *as1* genes are not allelic.

Staging of *pam1* meiocytes permits analysis of early meiotic prophase: The initial studies of the pam1 phenotype (Golubovskaya and Mashnenkov 1977; Golubovskaya 1989; Golubovskaya *et al.* 1994) suggested that the lesion responsible for defective synapsis may precede synapsis. To investigate this possibility we used 3-D deconvolution light microscopy to analyze FISH experiments with telomere, centromere, and 5S rDNA probes to describe the reorganization of the *pam1* nucleus during early prophase I.

The criteria outlined in Dawe *et al.* (1994) and Bass *et al.* (1997) were helpful for accuracy of staging of the prophase I nuclei in *pam1* meiocytes. Meiocytes were easily distinguishable from the much smaller tapetal cells. Meiocytes in interphase and leptotene had the same cell and nuclear size and the nucleolus was central in position in the nucleus, but the appearance of chromosomes was different in these two stages. The striking leptotene-zygotene transition stage could be distinguished from these other stages by differences in chromosome condensation, mainly by the elongation of the heterochromatic regions, such as knobs and pericentric heterochromatin, and by changes in polarization of chromosomes relative to the nucleolus. As described in Dawe *et al.* (1994) and Carlton and Cande (2002) these changes take place as pairing is initiated. Zygotene and pachytene chromosomes can be distinguished by their different morphology due to the extent of synapsis. Also, the space between individual chromosomes is less in zygotene than in pachytene. In addition to chromosome morphology, for staging we also took into account anther size, which can be correlated with meiotic stage. Finally, since progress through meiosis occurs in a developmental gradient on the tassel branch, we also allowed for relative floret position on the tassel in our staging. These later criteria are especially useful in the mutant since staging of *pam1* meiocytes can be a problem at pachytene because of the lack of synapsis. Differences in cell size, chromosome morphology, and the more dispersed chromosome distribution in the pachytene nucleus compared to those in the zygotene, however, allowed these two stages in the mutant to be distinguished.

TABLE 2

Meiotic telomere behavior in *pam1* mutants and wild-type siblings: number of cells found in each telomere clustering class

	Wild type					*pam1* mutant				
Genotype stage	L	L-Z	Z	Z-P	P	L	L-Z	Z	Z-P	P
Telomere status										
1. Telomeres spread out inside nucleus	7	0	0	0	0	12	0	0	0	0
2. Telomeres tether to NE or rim-like distribute on NE	3	1	0	0	0	9	6	10	3	1
3. Bouquet imperfect: loose bouquet, some telomeres outside bouquet, or a few clusters of telomeres	0	0	6	4	0	0	1	16	2	13
4. Perfect bouquet	0	0	24	1	0	0	0	5	0	1
5. Dissociated bouquet										
A. Completely	0	0	0	1	27	0	0	1	0	8
B. Incompletely	0	0	0	0	13	0	0	0	0	0
Total	10	1	30	6	40	21	7	32	5	23

Underlined numbers on the left side of table show dramatic changes in telomere clustering in prophase I in normal meiosis. Underlined numbers on the right side of table show inhibition of meiotic telomere movement in *pam1* meiocytes. L, leptotene; L-Z, leptotene-zygotene transition; Z, zygotene; Z-P, zygotene-pachytene; P, pachytene.

The *pam1* mutant is delayed in meiotic prophase: *pam1* was previously shown to possess multiple meiotic defects, including a notable asynchrony of meiocytes. Within single anthers, meiocytes were present in many different stages of meiosis, from zygotene to tetrads (Golubovskaya and Mashnenkov 1977). To determine whether asynchrony was still a prominent feature of the *pam1* mutant after long-term propagation, we confirmed this phenotype by examining meiocytes from seven anthers that developmentally should contain only tetrad stage meiocytes. The spectrum of stages from each individual anther was identical, so only the pooled data are reported here. A total of 366 meiocytes were analyzed and scored for their meiotic stage: 160 (43.7%) meiocytes reached the tetrad stage; 70 (19.1%) meiocytes were in meiosis II (prophase II to telophase II); 23 (7.0%) meiocytes were in the first meiotic division (metaphase I to dyads); and 113 (30%) meiocytes had not progressed further than prophase I (zygotene-diakinesis). Thus, some meiocytes had completed meiosis and reached the microspore stage (44%) and some (56%) did not, but all formed pollen walls at the developmentally appropriate time. As a result, mature anthers contained microspores that ranged fourfold in size. This range of sizes corresponded to the size of the cell when pollen wall formation was initiated. Mutant plants are completely male sterile, however, indicating that the population of meiocytes (44%) that appeared to complete the meiotic divisions was not viable. Because we used fixed material, we cannot distinguish between a population of meiocytes that arrest at various stages of meiotic prophase and remain at that stage, compared to a population of meiocytes that progress at various rates through meiosis.

Telomere bouquet clustering is inhibited in *pam1*: To study telomere clustering in the *pam1* mutant as compared to wild-type sibling plants during prophase I we did experiments using FISH with telomere-specific probes. In total, 88 *pam1* and 87 wild-type prophase I nuclei were analyzed. We observed several classes of the telomere associations: (1) telomeres freely scattered throughout the whole volume of the nucleus; (2) telomeres on the periphery of the nucleus presumably tethered to the NE (these telomeres form a rim-like distribution in any one optical section and although not clustered together are usually confined to one hemisphere); (3) imperfect bouquet, *i.e.*, a loose bouquet, a bouquet with a significant number (5–10) of telomeres outside the bouquet, or a few miniclusters of telomeres on the NE; (4) a perfect bouquet; and (5) a bouquet starting to dissociate at pachytene. Class 5 could be distinguished from class 3 by the relevant chromosome morphology. These classes represent a temporal sequence in telomere organization. The number and stage of meiocytes found in each class are summarized in Table 2 and these data are further described according to meiotic stage:

Leptotene: At leptotene, telomeres of both genotypes had the same distribution pattern; telomeres were freely scattered throughout the entire volume of the nucleus (Figures 1A and 2A). In some leptotene cells, telomeres were found close to the nuclear envelope.

Leptotene-zygotene transition: Seven cells were observed at this stage in *pam1* meiocytes. Only one meiocyte at this stage was found in the wild-type sibling population, although a similar number of meiotic cells were analyzed. The telomeres of both genotypes at this stage were near the periphery of the nucleus (Figures 1B and

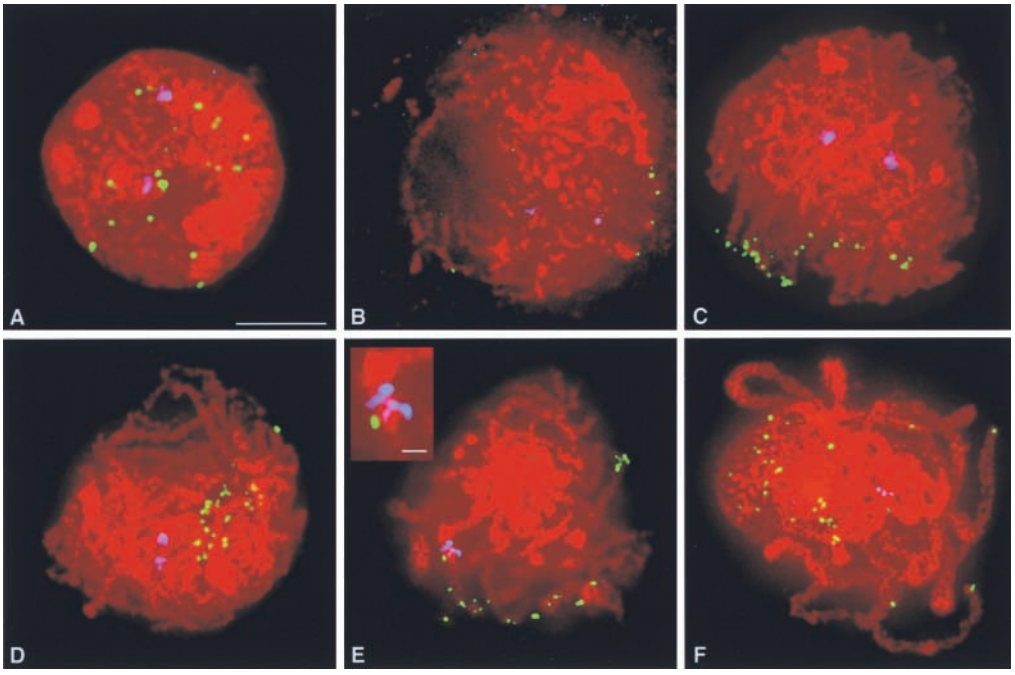

FIGURE 1.—Telomere distribution in wild-type sib maize meiocyte nuclei in leptotene through pachytene stages. The images are 2-D projections of complete 3-D image stacks of whole nuclei, unless otherwise noted. Chromosomes (DAPI) are shown in red, telomeres (FITC) in green, and 5S rDNA loci (Cy5) in blue. (A) Leptotene. Telomeres are randomly distributed throughout the nucleus. The two unpaired 5S rDNA loci are far away from each other. (B) Leptotene-zygotene transition (a one-tenth projection, showing only a few telomeres, is displayed). Telomeres are near the nuclear envelope (NE); the two 5S rDNA loci remain unpaired. (C) Zygotene. Telomere clustering is in progress and two unpaired 5S rDNA foci are visible; the right 5S rDNA locus is seen as a double spot, because the two sister chromatids have undergone a slight separation. (D) Zygotene. A tight telomere bouquet is visible and the two unpaired 5S rDNA foci are closer to each other. One telomere is outside of the bouquet. (E) Middle pachytene. A one-tenth projection is shown to display clearly the 5S rDNA signal rather than all the telomeres. Dissociation of the telomere bouquet cluster has been initiated and the pairing of two 5S rDNA foci is in progress. The morphology of the 5S rDNA loci is like a band wrapping around each homologous chromosome (see inset for detail). (F) Pachytene. The telomere bouquet is dissociated and the 5S rDNA loci are completely paired. Bar, 5 μm; A–F are same magnification; bar (inset in E), 1 μm.

3). In the wild-type nucleus, the telomeres were in a rim-like distribution. Six of the seven *pam1* nuclei had a similar morphology; the telomeres were in a rim-like configuration and were confined to one nuclear hemisphere (Figure 3, A–C). In one *pam1* nucleus, however, the telomeres were localized to a small region of the NE and formed a loose bouquet (Figure 3, D–F). At this stage in *pam1,* all 40 telomeres could be detected by the FISH probe. Some telomeres were seen as double spots with rod-shaped "stitches" between them, possibly indicating the beginning of synapsis (Figure 3).

Zygotene: Telomere behavior at the zygotene stage was very different in wild-type and *pam1* mutant plants (Table 2). A tight telomere bouquet was observed in 80% of the wild-type nuclei at zygotene (Figure 1, C and D). Other wild-type cells had a tight telomere bouquet but as has previously been shown, one or two telomeres were outside of the bouquet. One wild-type nucleus contained several miniclusters of telomeres and was likely undergoing the transition to pachytene. Although homologous synapsis was not yet complete, the dissociation of telomeres from the bouquet may have been initiated (Figure 1E). The pattern of telomere distribution in the *pam1* zygotene nuclei was dramatically different from the wild-type cells. An intermediate type of telomere clustering was often observed; 31% of the zygotene nuclei exhibited a rim-like pattern of telomere distribution (Table 2; Figure 2, B and C). Of the *pam1* zygotene meiocytes, 54% exhibited abnormal telomere clustering: either a loose bouquet, an incomplete bouquet in which several telomeres (3–10) were outside of the bouquet (Figure 2, D and E), or several miniclusters (data not shown). Only 15% of the zygotene meiocytes exhibited a tight bouquet.

Pachytene: The telomere behavior at pachytene was also different in wild-type as compared to *pam1* mutant meiocytes. Sixty-eight percent of the wild-type pachytene cells had no bouquet, presumably because the dissociation of the telomere bouquet initiated at the end of zygotene was complete. The remaining pachytene nuclei had small clusters of telomeres (Table 2; Figure 1F). This is probably an intermediate step in telomere dissociation. In most *pam1* mutant meiocytes the telomere configuration at the pachytene stage was similar to that in zygotene (Table 2; Figure 2, E and F). Thirty-five percent of the *pam1* nuclei showed the dispersed telomere pattern (data not shown), which could be due either to an arrest at the early stages of bouquet formation or to the dispersal of telomeres that normally occurs in pachytene.

Telomere-centromere polarization is normal in *pam1* nuclei: To observe the effect of the *pam1* mutation on centromere distribution in early prophase I nuclei, we performed 3-D FISH using a centromere-specific probe. No differences in the behavior of the centromeric regions in the *pam1* mutant compared to those in wild-

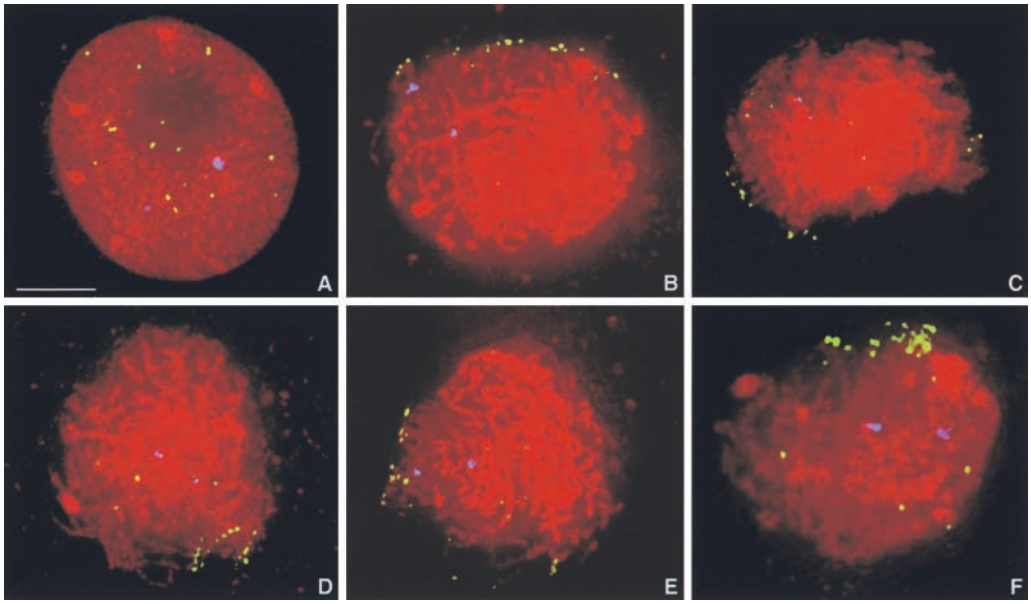

FIGURE 2.—*pam1* maize meiocyte nuclei in leptotene through pachytene stages. The images are 2-D projections of complete 3-D image stacks of serially sectioned nuclei, unless otherwise noted. Chromosomes (DAPI) are shown in red, telomeres (FITC) in green, and 5S rDNA loci (Cy5) in blue. (A) Leptotene. Telomeres are randomly distributed throughout the nucleus and two unpaired 5S rDNA loci are visible. Telomere behavior is similar to wild-type sibs at this stage. (B and C) Zygotene. These two nuclei, on the basis of their chromosome morphology, have progressed into zygotene (compare Figures 1D and 2B, for example), but telomere clustering is delayed at an intermediate stage. Telomeres are located on the NE and display a rim-like pattern of distribution but have not clustered. Two unpaired 5S rDNA foci (two blue spots) are seen in each nucleus. (D and E) Zygotene. These nuclei have imperfect telomere bouquets with some telomeres outside the cluster. Two unpaired 5S rDNA loci are seen as double spots in each nucleus. (F) Pachytene. A telomere bouquet is still present and all but five telomeres are in the bouquet. Two unpaired 5S rDNA loci are visible. In contrast, in wild-type sib nuclei the telomeres are dispersed and two 5S rDNA foci have undergone synapsis (compare to Figure 1F). Bar, 5 μm.

type meiocytes were observed. During the leptotene-zygotene transition *pam1* cells exhibited the typical centromere-telomere polarization that is observed in wild-type maize (CARLTON and CANDE 2002). An example of this can be seen in Figure 3. In one nucleus, all telomeres were on the nuclear periphery in one hemisphere of the nucleus and all centromeres but one were located in the opposite hemisphere (Figure 3, A–C). In the other nucleus, the telomeres formed a loose bouquet in the left hemisphere of the nucleus (Figure 3D), while the centromeres are located in the right hemisphere (Figure 3F). Neither telomeres nor centromeres are found in the middle of this nucleus (Figure 3E).

Synapsis of homologous chromosomes in the *pam1* mutant is aberrant: Transmission electron microscopy of silver-stained synaptonemal complex spreads was used to characterize the extent of synapsis in *pam1* as compared to wild-type meiocytes. A total of 25 pachytene nuclei from three *pam1* mutant plants and 15 wild-type pachytene nuclei from one wild-type sibling were studied.

All *pam1* nuclei had abnormal chromosome synapsis in pachytene. In some nuclei, the extent of synapsis appeared to be similar to wild type and only the presence of chromosomes switching synaptic partners indicated that nonhomologous chromosome synapsis occurred (Figure 4A). In other *pam1* pachytene nuclei, prominent defects were observed including incomplete synapsis, as determined from regions of unsynapsed chromosomes, and nonhomologous synapsis, either in the form of chromosomes folding back on themselves (fold backs) or in the form of chromosomes switching pairing partners along their length. Both terminal and interstitial regions of chromosomes could be involved in nonhomologous synapsis (Figure 4, B–D). In most pachytene nuclei, only one to three partner-switching events occurred. Unresolved chromosome interlocks (two or more chromosomes entangled and unable to resolve) during pachytene were also observed (Figure 4E).

Wild-type meiocytes at pachytene exhibited complete homologous synapsis (Figure 4F). Neither fold backs and pairing partner switches characteristic of nonhomologous synapsis nor univalent chromosomes were observed, although some short regions at distal ends of chromosomes could be unsynapsed (image not shown). Unresolved chromosome interlocks were never observed.

Homologous synapsis of 5S rDNA locus (2L) is decreased in *pam1* nuclei: To determine the extent of homologous pairing at a single gene locus in *pam1* compared to wild-type sibling maize meiocytes, we used FISH and a probe that would identify the 5S rDNA loci during leptotene, zygotene, and pachytene (Table 3). The 5S rDNA locus maps on the distal side of the long arm of maize chromosome 2 (bin 2.08). In wild-type maize meiocytes at leptotene the two 5S rDNA loci are unpaired and usually far apart (Table 3; Figure 1A). Each homologous locus is often visible in FISH as double spots, corresponding to the two sister chromatids. In ~50% of the zygotene nuclei, two 5S rDNA loci are seen, often close to each other. In the other half of the zygotene meiocytes, only one large bright 5S rDNA spot

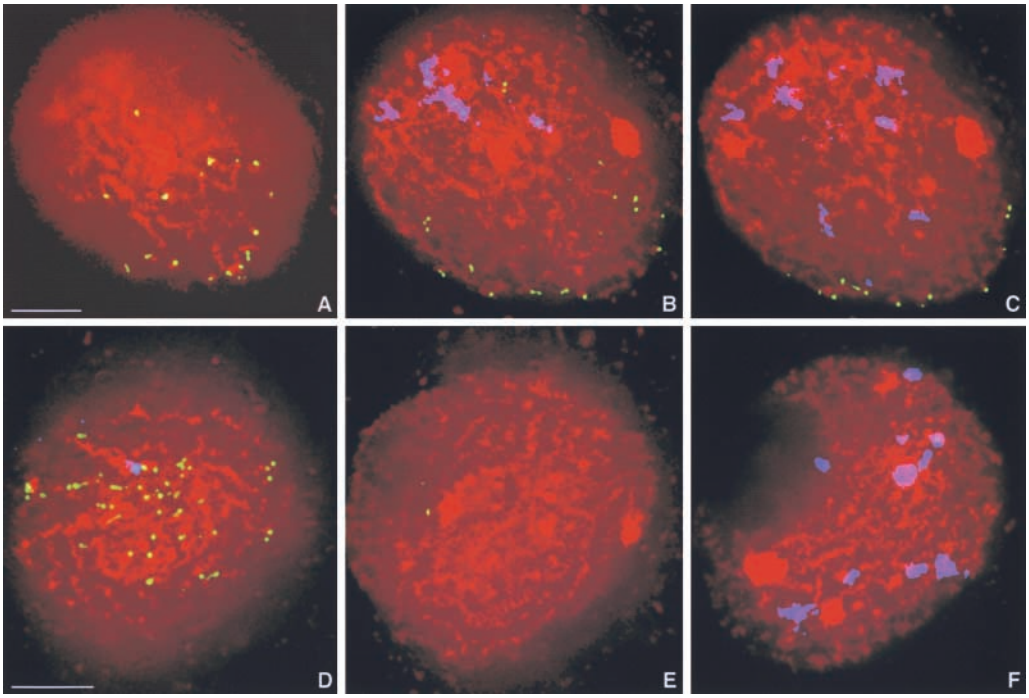

FIGURE 3.—Telomere distribution and polarization of telomeres and centromeres at leptotene-zygotene transition in *pam1* nuclei. Two nuclei are displayed as a series of sequential one-third volume projections (A, B, C and C, D, E). Chromosomes (DAPI) are shown in red, telomeres (FITC) in green, and centromeres (Cy5) in blue. (A–C) In the first nucleus, all 40 telomeres can be distinguished and some of them are seen as doublets. Centromeres (upper hemisphere) and telomeres (lower hemisphere) are located at opposite ends of the nucleus. (A) Only telomeres attached to the edge of the nuclear envelope (NE) are seen. (B and C) Telomeres are mostly located on the edge of the NE, but some are internal. (D–F) Second nucleus. Polarization between telomeres and centromere regions at the leptotene-zygotene transition stage can be observed. (D) Most of the telomeres are in a loose cluster on the surface of the NE in this one-third projection. Some telomeres are seen as doublets and others as single spots connected by stitches. Only one centromere (blue spot) is seen in this projection. (E) Two telomeres are seen in the middle of the nucleus. (F) All centromeres but one are seen in this final projection of the nucleus, and most of the centromeres are near the NE. Bars, 5 μm.

was visible, most likely indicating synapsed 5S rDNA loci. One 5S rDNA locus was always seen in late zygotene and pachytene (Table 3; Figure 1, E and F) when homologous synapsis is complete.

The 5S rDNA loci in *pam1* mutant meiocytes at leptotene were distributed spatially similar to those in wild-type leptotene. During the remainder of prophase I the behavior of the 5S rDNA loci was very different in *pam1* meiocytes in comparison with wild type (Table 3; Figure 2). During the leptotene-zygotene transition and zygotene, the 5S rDNA loci were synapsed in only 1 of the 27 *pam1* meiocytes examined. At pachytene, 59% of the *pam1* nuclei contained unsynapsed 5S rDNA loci. Because we examined fixed material, we cannot determine whether this is due to a general retardation of homologous synapsis or whether homologous synapsis has arrested at an early stage, while chromosome condensation continued.

Distribution of RAD51 foci is normal in *pam1* during prophase I: The RecA homolog, RAD51, performs a central role in catalyzing the DNA strand exchange event of meiotic recombination and may also be involved in homolog recognition. During meiosis in maize, RAD51 foci form on unpaired chromosomes and then disappear as chromosomes synapse except at a few sites where reciprocal recombination may be taking place (FRANKLIN *et al.* 1999). It is possible that some of the defects in chromosome behavior we observed in *pam1* meiocytes could be explained by an altered distribution of RAD51 foci in these cells compared to that in wild-type cells. We used RAD51 antibodies and 3-D immunofluorescence microscopy to analyze the distribution of RAD51 foci *pam1* meiocytes (Table 4; Figure 5). The RAD51 protein was diffuse within meiocyte nuclei during leptotene in both *pam1* mutants and their wild-type siblings. At the zygotene stage, the RAD51 protein formed distinct foci on chromosomes. The foci were spread throughout the nucleus and their pattern of distribution was similar in *pam1* and wild-type meiocytes. There was little difference in the average number of foci at midzygotene between mutant and wild-type cells. The level of the RAD51 protein in zygotene anthers, as measured by Western blot analysis, was also similar (data not shown). The number of RAD51 foci decreased toward the end of zygotene in both *pam1* and wild-type meiocytes, although the number of RAD51 foci remaining at pachytene was greater in *pam1* than in wild-type nuclei (Table 4; Figure 5, compare C and G). RAD51 foci disappeared in both genotypes at late pachytene just before diplotene (Figure 5D).

DISCUSSION

Initiation of bouquet formation is normal in *pam1* meiocytes: Organisms differ in the timing of bouquet formation during meiosis. In some species such as bud-

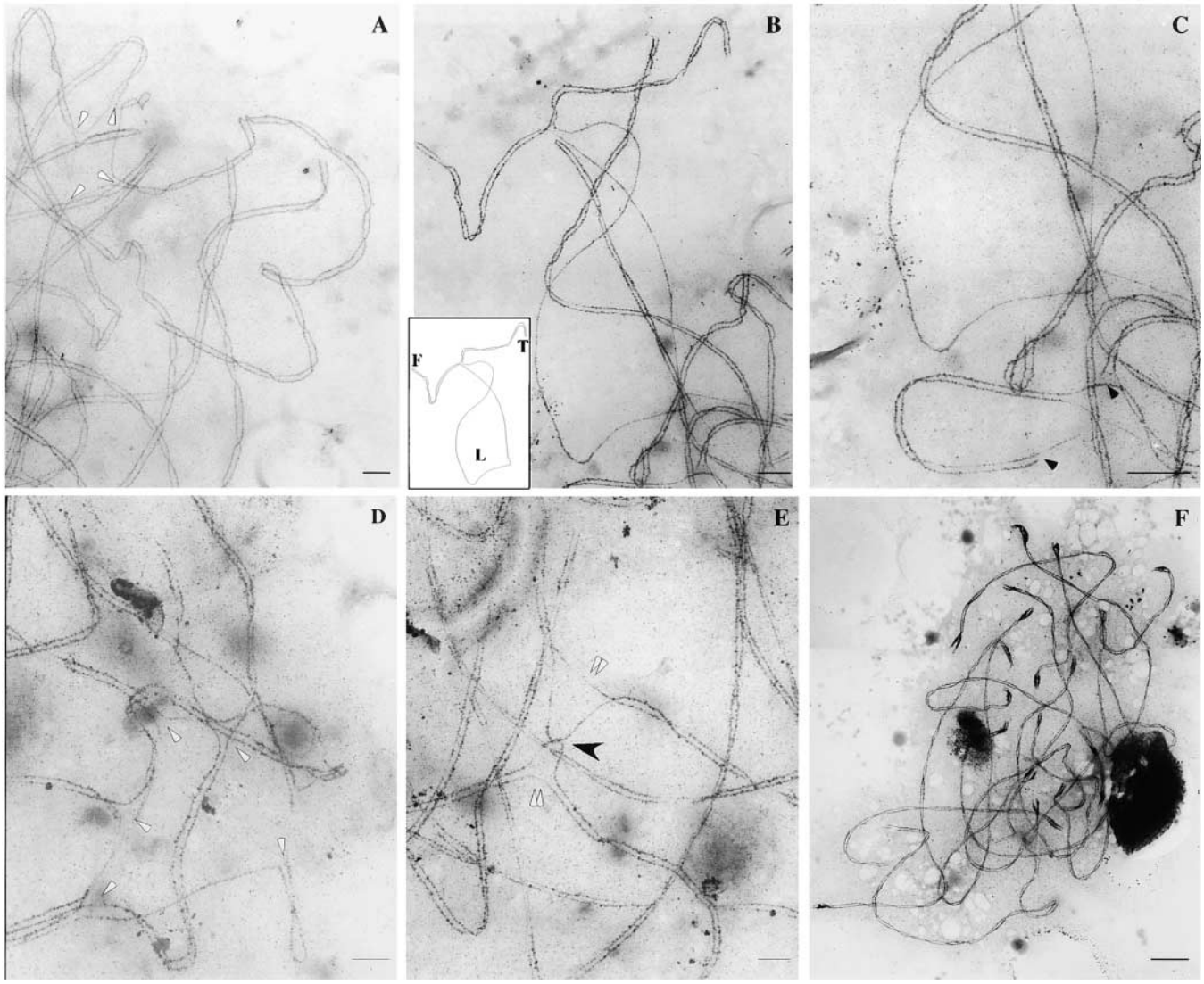

Figure 4.—TEM of chromosome synapsis in nuclei whose chromosomes were spread and stained with silver nitrate. (A–E) *pam1* and (F) wild-type sibs. (A) A part of a *pam1* pachytene nucleus with extensive synapsis. Switching of the synaptic partners (white arrowheads) indicates the presence of nonhomologous synapsis. (B) A region of a *pam1* pachytene nucleus. Univalent chromosome displays nonhomologous synapsis and is diagrammed in inset. The tips of both arms of the univalent chromosome are synapsed and marked with the letter T. An interstitial region of the univalent chromosome involved in a fold-back synapsis is marked with the letter F. An interstitial unsynapsed chromosome region forming a loop is marked with the letter L. (C) Another region of the same pachytene nucleus; nonhomologous synapsis involving both terminal and interstitial regions is marked with black arrowheads. (D) Region of a pachytene *pam1* nucleus with numerous nonhomologous synapses (white arrowheads). (E) Region of a pachytene nucleus with an unresolved interlock (black arrowhead) and lack of synapsis near the interlock (double white arrowheads). (F) Region of a wild-type pachytene nucleus with complete homologous synapsis. Bars: A–E, 500 nm; F, 2 μm.

ding yeast, fission yeast, and several species of higher plants, telomere clustering starts in premeiotic interphase or even earlier (Cooper *et al.* 1998; Trelles-Sticken *et al.* 1999; Martinez-Perez *et al.* 2000; Scherthan 2001). In other species such as human, mouse, rye, and maize, telomere reorganization starts *de novo* at the leptotene-zygotene transition (Bass *et al.* 1997; Scherthan *et al.* 2000; Cowan and Cande 2002). But in all cases, the chromosomes ends, irrespective of their arm length, become directly attached to the inner membrane of the NE. The chromosomes are strongly polarized and form loops extending into the center of the nucleus (Zickler and Kleckner 1998). Our previous analysis of bouquet formation in maize using chromosome derivatives such as ditelocentrics and ring chromosomes demonstrates that this process is telomere driven and does not require a chromosome physical end. This suggests that formation of the bouquet may require only the telomeric repetitive sequence (Carlton and Cande 2002).

The initiation of telomere clustering and initiation of synapsis of homologous chromosomes coincide with

TABLE 3

Pattern of synapsis in 5S rDNA loci in *pam1* and wild-type meiocytes

	Stages of meiosis											
	L		L-Z		Z		Z-P		P		Total cells	
Genotype	s	u	s	u	s	u	s	u	s	u	s	u
Wild type	0	10	0	0	14	16	6	0	39	1	59	27
pam1 mutant	0	16	0	7	1	20	1	4	7	10	9	57

s, synapsed 5S rDNA foci (1 signal is seen); u, unsynapsed 5S rDNA foci (2 signals are seen); L, leptotene; Z, zygotene; P, pachytene.

the leptotene-zygotene transition (Loidl 1990; Bass *et al.* 1997; Zickler and Kleckner 1998). During this brief but recognizable stage, telomeres appear to attach to the NE. In a subsequent and separate step, telomeres coalesce into a tight cluster, which is coincident with entry into zygotene (Bass *et al.* 1997, 2000). In wild-type maize meiocytes, the telomeres apparently start to aggregate immediately after attachment to the NE. We have called this an "early bouquet" (see Bass *et al.* 1997).

The kinetics of wild-type telomere clustering compared to that of *pam1* is displayed in Figure 6. The localization or attachment of telomeres to the inner NE is spatially and temporally normal in the *pam1* mutant. Heterochromatic knobs and centromeric heterochromatin have compact shapes on maize leptotene chromosomes but elongate and change shape during the leptotene-zygotene transition. At this particular stage, telomere regions visualized by FISH appear as double spots, as telomeres from homologous arms approach each other on the NE (Dawe *et al.* 1994; Carlton and Cande 2002). These changes are found in both *pam1* and wild-type chromatin. In maize, telomeres and centromeres are located in opposite hemispheres of the meiocyte nucleus at the beginning of the leptotene-zygotene transition (Carlton and Cande 2002). In the *pam1* mutant a similar polarization of telomeres and centromeres occurs.

Inhibition of telomere clustering is the earliest lesion detected in the *pam1* mutant: The inability of *pam1* meiocytes to make a normal telomere bouquet in a timely fashion is the earliest detectable phenotype in this mutant, and the leptotene-zygotene transition is the earliest stage in which we could detect abnormal telomere behavior. Telomeres in *pam1* nuclei appeared to be blocked in telomere clustering rather than in the steps required for telomere localization to the nuclear periphery and attachment to the NE. On the basis of these observations, we suggest that the function of wild-type *pam1* is required for movement of the telomeres on the NE rather than their association with the NE (Figure 6).

In *pam1*, the association of telomeres with the NE appears to be initiated at the right time, but subsequent progress is severely delayed or arrested before telomeres successfully cluster. Since we analyzed only fixed cells, it is not possible to determine whether telomere movement is arrested at different stages in different cells or whether it occurs at different rates in various cells and shows variable progress when the cells are fixed. In any

TABLE 4

Distribution of RAD51 foci in prophase I of meiosis in wild-type maize and the *pam1* mutant

Genotype and stages of meiosis	No. of studied cells	RAD51 foci		
		No. of foci	Mean	SD
Wild type				
Leptotene	10	0–2	0.5	1
Zygotene	25	150–624	386	141
Zygotene-pachytene	12	86–141	119	22
Pachytene	10	5–30	12	8
Late pachytene	8	0	0	0
pam1 mutant				
Leptotene	9	0–3	0.6	1
Zygotene	34	210–437	347	66
Zygotene-pachytene	10	143–296	201	75
Late pachytene	6	0–2	0.3	0.5

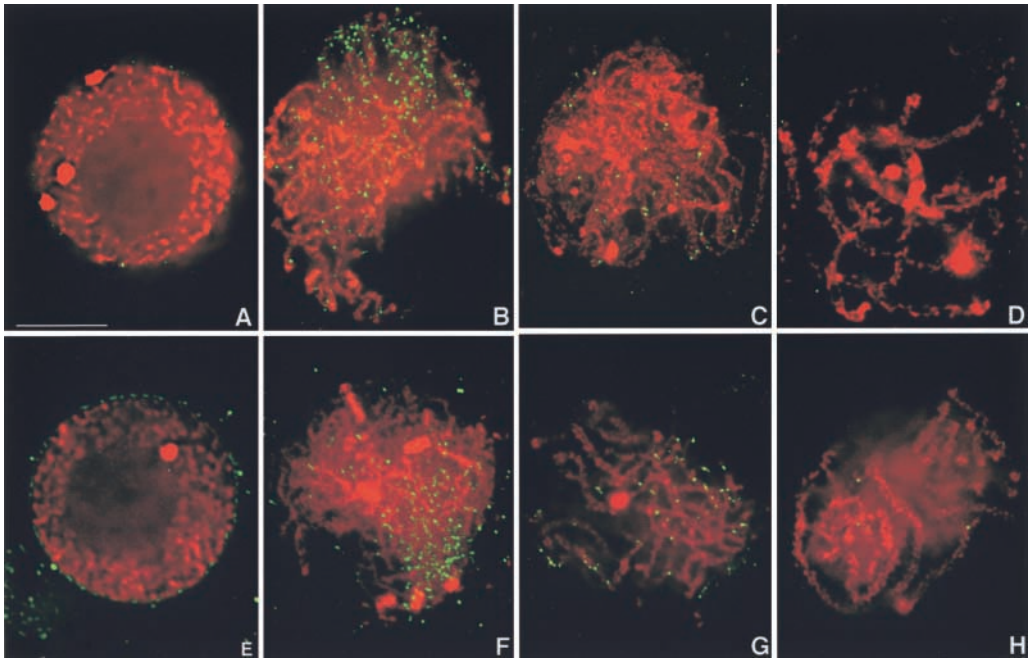

FIGURE 5.—Distribution of RAD51 foci during leptotene through pachytene stages in wild-type sibs and *pam1* nuclei. The images are flat projections of complete 3-D image stacks of serially sectioned nuclei, unless otherwise noted. Chromosomes (DAPI) are shown in red, and RAD51 foci immunostained with anti-Hs RAD51(FITC) are shown in green. Partial nuclei are shown to more clearly display synapsed *vs.* unsynapsed chromosome regions. (A–D) Wild-type nuclei. (A) Leptotene. No visible RAD51 foci are on leptotene chromosomes. RAD51 foci staining outside of NE represents either nonspecific AbRAD51 binding or RAD51 protein on the surface of the nucleus (FRANKLIN *et al.* 1999). (B) Zygotene. Numerous RAD51 foci are located on zygotene chromosomes. (C) Middle pachytene. Decreased numbers of RAD51 foci (~40 foci) are located on pachytene chromosomes. (D) Late pachytene (partial nuclear projection). No RAD51 foci are observed on pachytene chromosomes. (E–H) *pam1* nuclei. (E) Leptotene. No RAD51 foci are on leptotene chromosomes, as in wild type. (F) Zygotene. Many RAD51 foci are seen on *pam1* chromosomes, in similar numbers to wild type. (G) Middle pachytene (partial nuclear projection). Decreased numbers of RAD51 foci are seen on pachytene chromosomes. (H) Late pachytene (partial nuclear projection). Only a few RAD51 foci are found and they are on synapsed regions of chromosomes. Bar, 5 μm.

case, it is clear that most *pam1* meiocytes do not have a tight bouquet in zygotene at the onset of synapsis. Our analysis of bouquet formation in these mutant cells indicates that telomeres cluster slowly throughout zygotene. Only a few cells at zygotene have a complete bouquet; most are in an intermediate stage. In *pam1* mutants, the rim-like stage of telomere clustering on NE sometimes persisted into pachytene. While this is a feature of the leptotene-zygotene transition, it is not seen later in prophase in wild-type cells (Table 2; Figure 6).

In summary, three categories of imperfect bouquet were found in *pam1* meiocytes: (1) several miniclusters (Figure 2, B and C), (2) a tight bouquet but a significant number of telomeres remaining in the nuclear interior (Figure 2E), and (3) a loose bouquet (Figure 3D). We speculate that these stages may be intermediates in the normal telomere clustering process, and we cannot find them in wild-type meiocytes because they are transient. Alternatively, these could be aberrant bouquets found only in the *pam1* meiocyte.

Homologous synapsis is not accomplished efficiently in *pam1*: Pairing and synapsis are aberrant in *pam1* meiocytes. We used FISH probes against the 5S rDNA locus to monitor the pairing of a single locus during zygotene. The 5S rDNA loci remained mostly unpaired throughout zygotene and only ~41% of the foci were paired in pachytene. In contrast, in wild-type sibs 50% of the foci were paired by zygotene and 100% were paired in pachytene. Transmission electron microscopy of the spread whole nuclei revealed many synaptonemal defects in *pam1* pachytene nuclei. Apparently homologous synapsis was accompanied by unsynapsed univalent chromosomes and by nonhomologous synapsis. The nonhomologous synapsis could be the result of synapsis of univalent chromosomes to themselves as well as nonhomologous synapsis of different chromosomes. In the latter case, both interstitial regions and terminal regions of nonhomologous and homologous chromosomes could be involved in synapsis (Figure 4, B and C). Although a few nuclei had numerous regions involved in nonhomologous synapsis (Figure 4D), in most nuclei the number of nonhomologously synapsed regions was limited and there were only one to three partner exchanges per cell (compare Figure 4A with 4D). In addition to nonhomologous synapsis, unresolved interlocks were found. These were also not observed in wild-type nuclei.

Failure to form a bouquet leads to defects in homologous synapsis: We interpret the failure to pair and synapse properly in the *pam1* mutant to be a consequence of the failure to form a wild-type bouquet. Other aspects of meiocyte development proceed in *pam1* as in wild type, including stage-specific changes in cell size, nuclear volume, position of the nucleolus, and chromatin

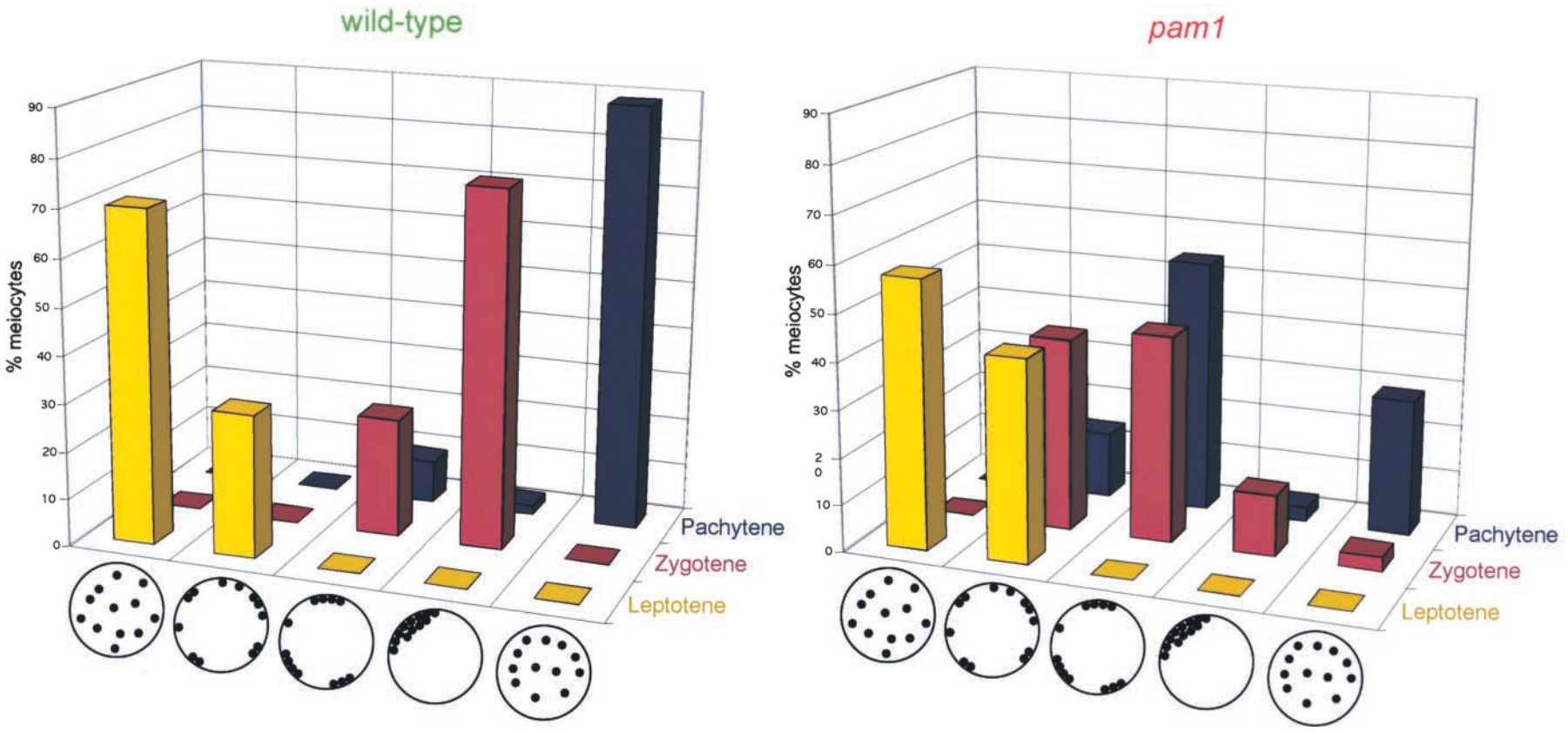

FIGURE 6.—Telomere behavior in meiotic prophase in *pam1* mutant *vs.* wild-type meiocytes. The 3-D bar graphs illustrate the progress of telomere reorganization during early prophase. The data from Table 2 were used to create the graphs. To simplify visualization of *pam1* telomere behavior we lumped leptotene-zygotene and zygotene-pachytene transition stages with leptotene and pachytene, respectively. Horizontal axis shows five classes of telomere organization, from left to right: (1) telomeres freely scattered in the entire volume of the nucleus; (2) telomeres located on the inner surface of NE in a rim-like configuration; (3) telomeres at an intermediate stage of bouquet formation, showing loose clusters and/or miniclusters; (4) tight bouquet; and (5) telomeres dispersing from the bouquet. The wild-type graph (left) shows normal reorganization of telomeres from leptotene through pachytene. *pam1* graph (right) shows delay in telomere reorganization from leptotene to pachytene. Telomere behavior in the *pam1* mutant is similar to the wild type at leptotene stage. Telomere movement is inhibited at the intermediate stage of telomere clustering and, as a result, the majority of cells show rim-like configuration of the telomeres at zygotene. The intermediate bouquet stage persists in a majority of cells during pachytene. A few cells form a perfect bouquet, and a few cells show dispersion of telomeres from a bouquet.

condensation state. The distribution of RAD51 foci in *pam1* nuclei is similar to that in wild-type cells, suggesting that the molecular machinery responsible for determining homology and required for meiotic recombination is unaffected by *pam1*. Those processes most affected by *pam1* may be the events most influenced by the lack of directed chromosome movement in the prophase nucleus. These could include failure to bring homologous chromosomes into close proximity to each other and align them appropriately and failure to develop the tension that may be required to regulate processes such as chromosome interlock resolution.

It was proposed that dissociation of telomere bouquet is also important for proper homologous synapsis, and any delay in dissociation of the telomere clusters could result in improper synapsis because of restriction in the mobility of chromosomes (Zickler and Kleckner 1998). Our TEM of *pam1* pachytene chromosomes is in agreement with this proposal. The pattern of nonhomologous synapsis and univalent chromosome displayed in Figure 4B indicates that telomeres of the two arms of the chromosome attached to the NE could not separate from each other because of the arrest of telomere clustering. Nonhomologous chromosomes may also interact with each because they are in close juxtaposition and cannot move away to find their appropriate partner.

Several lines of evidence support our argument that the failure to form a bouquet leads to incomplete and nonhomologous synapsis. First, defects in telomere clustering known in other organisms causes improper synapsis, delayed meiosis, decreased recombination, and infertility. Fission yeast mutants deficient for TAZ1, a protein required for maintenance of telomere repeat sequence length, exhibit improper telomere clustering with the spindle pole body during meiotic prophase (Cooper *et al.* 1998). Recombination in this mutant is reduced three- to fourfold compared to wild-type cells. Thus, reorganization of the fission yeast nucleus during meiotic prophase is required for facilitating chromosome synapsis and recombination (Chua and Roeder 1997; Nimmo *et al.* 1998). In the budding yeast *ndj1* mutant, telomeres are dispersed in the nucleus and never attach to the NE, and thus bouquet formation does not occur. Subsequently, there is a delay in the onset and completion of synapsis, nonhomologous synapsis, decreased recombination, and severe sterility (Chua and Roeder 1997; Conrad *et al.* 1997; Trelles-Sticken *et al.* 2000). *pam1* also affects homologous synapsis and recombination; however, in contrast to these and other bouquet mutants, *pam1* is the only mutant that we know of that affects telomere movement on the NE rather than telomere localization or attachment to the NE. Our study is also the first demonstration that telomere attachment to the NE and subsequent telomere clustering are genetically distinct steps.

Second, we have shown that colchicine blocks telomere clustering in rye meiocytes (Cowan and Cande 2002). Colchicine treatment appears to phenocopy the *pam1* mutation. When applied to plants and animals early in meiotic prophase, colchicine is known to cause improper synapsis, decreased chiasmata formation, and frequency of recombination leading to univalent chromosomes followed by infertility (Shepard *et al.* 1974; Thompson and Ingraham 1986; Loidl 1988; Tepperberg *et al.* 1997). It has been shown for higher plants and for mouse that the leptotene-zygotene transition seems to be the crucial stage at which colchicine treatments have their effect and that treatment with colchicine after zygotene has no effect on meiosis (Shepard *et al.* 1974; Thomas and Kaltsikes 1977; Bennett *et al.* 1979; Toledo *et al.* 1979).

By adding colchicine to rye anthers in culture at various times during prophase I (leptotene through pachytene) and monitoring both stage and telomere distribution, we demonstrated that the colchicine specifically disrupts the movement of telomeres on the NE, but does not affect other nuclear reorganizations such as nuclear pore reorganization (Cowan and Cande 2002). Telomeres in colchicines-treated cells remained scattered in the nuclear periphery while control cells exhibited a prominent telomere cluster. Colchicine appears to inhibit lateral movement of telomeres on the NE rather than their association with the NE (Cowan and Cande 2002). Although we do not know whether these *in vitro* treatments interfere with synapsis, the inhibition of bouquet formation in rye anthers treated by colchicine is very similar to the block in bouquet formation in *pam1* meiocytes. The fact that colchicine blocks telomere clustering in this system and disrupts homologous synapsis in many other cell types is further evidence that the two processes are causally related.

Most meiotic mutants that are defective in synapsis and recombination have wild-type bouquets. The yeast *spo11* and *rad50*, maize *dsy1* and *dsy2*, and rye *sy9* are examples of genes that fall into this category (Loidl *et al.* 1994; Roeder 1997; Roeder and Bailis 1999; Trelles-Sticken *et al.* 1999; Mikhailova *et al.* 2001; our unpublished data). This observation suggests that the *pam1* gene and genes such as *taz1* and *ndj1* control a telomere-dependent pathway of homologous synapsis in which synapsis is downstream from bouquet formation. Defective bouquet formation, as seen in *pam1*, does not block other prophase I processes such as interlock resolution and homologous synapsis but rather makes them less efficient. This is evidenced by behavior of the 5S rDNA locus at pachytene (Table 3). In addition some *pam1* meiocytes in anthers completed meiosis and some megaspore mother cells even formed normal eight-nuclei embryo sacs after meiosis (Golubovskaya *et al.* 1994). Pollen walls form around microspores even though the cells are not viable. The continuation of other cellular

events during both meiosis and subsequent development is consistent with the hypothesis that *pam1* affects a step in bouquet formation rather than having a general effect on meiocyte metabolism. However, the striking asynchrony of pairing in anthers in the *pam1* meiocytes suggests that there are novel regulatory linkages in maize between bouquet formation and subsequent meiotic processes analogous to checkpoint control of cell cycle events described for other stages in the life cycle of maize and other organisms.

We are grateful to Z. K. Grbennikova for assistance with TEM study. We are grateful to Pete Carlton, Carrie Cowan, Scott Dawson, Satoru Uzawa, and Ye Jin for helpful discussions, comments on the manuscript, and emotional support. This research was supported by grants from the National Institutes of Health and Torrey Mesa Research Institute, Syngenta Research and Technology, San Diego.

LITERATURE CITED

Ananiev, E. V., R. L. Phillips and H. W. Rines, 1998 Chromosome-specific molecular organization of maize (*Zea mays* L.) centromeric regions. Proc. Natl. Acad. Sci. USA. **95:** 13073–13078.

Bass, H. W., W. F. Marshall, J. W. Sedat, D. A. Agard and W. Z. Cande, 1997 Telomeres cluster de novo before the initiation of synapsis: a three-dimensional spatial analysis of telomere positions before and during meiotic prophase. J. Cell Biol. **137:** 5–18.

Bass, H. W., O. Riera-Lizarazu, E. V. Ananiev, S. J. Bordoli, H. W. Rines *et al.*, 2000 Evidence for the coincident initiation of homolog pairing and synapsis during the telomere-clustering (bouquet) stage of meiotic prophase. J. Cell Sci. **113:** 1033–1042.

Beadle, G. W., 1930 Genetic and cytological studies of a Mendelian asynaptic in Zea Mays. Cornell Agric. Exp. Sta. Mem. **129:** 175–189.

Bennett, M. D., L. A. Toledo and H. Stern, 1979 The effect of colchicine on meiosis in Lilium speciosum cv. "Rosemeade." Chromosoma **72:** 175–189.

Carlton, P. M., and W. Z. Cande, 2002 Telomeres act autonomously in maize to organize the meiotic bouquet from a semipolarized chromosome orientation. J. Cell Biol. **157:** 231–242.

Chua, P. R., and G. S. Roeder, 1997 Tam1, a telomere-associated meiotic protein, functions in chromosome synapsis and crossover interference. Genes Dev. **11:** 1786–1800.

Conrad, M. N., A. M. Dominguez and M. E. Dresser, 1997 Ndj1p, a meiotic telomere protein required for normal chromosome synapsis and segregation in yeast. Science **276:** 1252–1255.

Cooper, J. P., E. R. Nimmo, R. C. Allshire and T. R. Cech, 1997 Regulation of telomere length and function by a Myb-domain protein in fission yeast. Nature **385:** 744–747.

Cooper, J. P., Y. Watanabe and P. Nurse, 1998 Fission yeast Taz1 protein is required for meiotic telomere clustering and recombination. Nature **392:** 828–831.

Cowan, C. R., and W. Z. Cande, 2002 Meiotic telomere clustering is inhibited by colchicine but does not require cytoplasmic microtubules. J. Cell Sci. **115:** 3747–3756.

Cowan, C. R., P. M. Carlton and W. Z. Cande, 2001 The polar arrangement of telomeres in interphase and meiosis. Rabl organization and the bouquet. Plant Physiol. **125:** 532–538.

Dawe, R. K., J. W. Sedat, D. A. Agard and W. Z. Cande, 1994 Meiotic chromosome pairing in maize is associated with a novel chromatin organization. Cell **76:** 901–912.

Dernburg, A. F., J. W. Sedat, W. Z. Cande and H. W. Bass, 1995 Cytology of telomeres, pp. 295–338 in *Telomeres*, edited by E. H. Blackburn and C. W. Grieder. Cold Spring Harbor Laboratory Press, Cold Spring Harbor, NY.

Dong, F., and J. Jiang, 1998 Non-Rabl patterns of centromere and telomere distribution in the interphase nuclei of plant cells. Chromosome Res. **6:** 551–558.

Franklin, A. E., J. McElver, I. Sunjevaric, R. Rothstein, B. Bowen *et al.*, 1999 Three-dimensional microscopy of the Rad51 recombination protein during meiotic prophase. Plant Cell **11:** 809–824.

Gelei, J., 1921 Weitere Studien uber die Oogenese des Dendrocoelum lacteum. II. Die Langskonjugation der Chromosomen. Arch. Zellforsch. **16:** 88–169.

Gillies, C. B., 1981 Electron microscopy of spread maize pachytene synaptonemal complexes. Chromosoma **83:** 575–591.

Golubovskaya, I., Z. K. Grebennikova, N. A. Avalkina and W. F. Sheridan, 1993 The role of the ameiotic1 gene in the initiation of meiosis and in subsequent meiotic events in maize. Genetics **135:** 1151–1166.

Golubovskaya, I. N., 1989 Meiosis in maize: *mei* genes and conception of genetic control of meiosis. Adv. Genet. **26:** 149–192.

Golubovskaya, I. N., and A. S. Mashnenkov, 1977 Multiple disturbances of meiosis in corn caused by a single recessive mutation pamA-A344. Genetika **13:** 1910–1921.

Golubovskaya, I. N., N. A. Avalkina and E. E. Peremyslova, 1994 Genes pam1 and pam2 control cytokinesis at different stages of development of maize sporogenous cells. Genetika **30:** 1392–1399.

Jin, Y., S. Uzawa and W. Z. Cande, 2002 Fission yeast mutants affecting telomere clustering and meiosis-specific spindle pole body integrity. Genetics **160:** 861–876.

John, B., 1990 *Meiosis* (Developmental and Cell Biology Series 22). Cambridge University Press, New York.

Laughnan, J. R., and S. Gabay-Laughnan, 1994 The placement of genes using waxy-marked reciprocal translocations, pp. 255–257 in *The Maize Handbook*, edited by M. Freeling and V. Walbot, Springer Verlag, New York.

Loidl, J., 1988 The effect of colchicine on synaptonemal complex formation in Allium ursinum. Exp. Cell Res. **178:** 93–97.

Loidl, J., 1990 The initiation of meiotic chromosome pairing: the cytological view. Genome **33:** 759–778.

Loidl, J., F. Klein and H. Scherthan, 1994 Homologous pairing is reduced but not abolished in asynaptic mutants of yeast. J. Cell Biol. **125:** 1191–1200.

Maguire, M. P., and R. W. Riess, 1991 Synaptonemal complex behavior in asynaptic maize. Genome **34:** 163–168.

Martinez-Perez, E., P. J. Shaw and G. Moore, 2000 Polyploidy induces centromere association. J. Cell Biol. **148:** 233–238.

Mikhailova, E. I., S. P. Sosnikhina, G. A. Kirillova, O. A. Tikholiz, V. G. Smirnov *et al.*, 2001 Nuclear dispositions of subtelomeric and pericentromeric chromosomal domains during meiosis in asynaptic mutants of rye (Secale cereale L.). J. Cell Sci. **114:** 1875–1882.

Nimmo, E. R., A. L. Pidoux, P. E. Perry and R. C. Allshire, 1998 Defective meiosis in telomere-silencing mutants of Schizosaccharomyces pombe. Nature **392:** 825–828.

Redei, G. P., 1998 *Genetic Manual*. World Scientific, Singapore.

Roeder, G. S., 1997 Meiotic chromosomes: it takes two to tango. Genes Dev. **11:** 2600–2621.

Roeder, G. S., and J. M. Bailis, 1999 The pachytene checkpoint. Trends Genet. **9:** 395–403.

Scherthan, H., 2001 A bouquet makes ends meet. Nat. Rev. Mol. Cell. Biol. **2:** 621–627.

Scherthan, H., M. Jerratsch, B. B. Li, S. Smith, M. Hulten *et al.*, 2000 Mammalian meiotic telomeres: protein composition and redistribution in relation to nuclear pores. Mol. Biol. Cell **7:** 4189–4203.

Shepard, J., E. R. Boothroyd and H. Stern, 1974 The effect of colchicine on synapsis and chiasma formation in microsporocytes of Lilium. Chromosoma **44:** 423–437.

Shimanuki, M., F. Miki, D. Q. Ding, Y. Chikashige, Y. Hiraoka *et al.*, 1997 A novel fission yeast gene, kms1+, is required for the formation of meiotic prophase-specific nuclear architecture. Mol. Gen. Genet. **254:** 238–249.

Tepperberg, J. H., M. J. Moses and J. Nath, 1997 Colchicine effects on meiosis in the male mouse. Chromosoma **106:** 183–192.

Thomas, J. R., and P. J. Kaltsikes, 1977 The effect of colchicine on chromosome pairing. Can. J. Genet. Cytol. **19:** 231–249.

Thompson, A. M., and R. Ingraham, 1986 The control of chiasma formation in colchicine-treated meiocytes of Senecio squalidis. Heredity **59:** 353–354.

Toledo, L. A., M. D. Bennett and H. Stern, 1979 Cytological investigations of the effect of colchicine on meiosis in Lilium hybrid cv. "Black Beauty" microsporocytes. Chromosoma **72:** 153–172.

Trelles-Sticken, E., J. Loidl and H. Scherthan, 1999 Bouquet formation in budding yeast does not require homologous chromosomes. J. Cell Sci. **112:** 651–658.

Trelles-Sticken, E., M. E. Dresser and H. Scherthan, 2000 Meiotic telomere protein Ndj1p is required for meiosis-specific telomere distribution, bouquet formation and efficient homologue pairing. J. Cell Biol. **151:** 95–106.

von Wettstein, D., S. W. Rasmussen and P. B. Holm, 1984 The synaptonemal complex in genetic segregation. Annu. Rev. Genet. **18:** 331–413.

Zickler, D., and N. Kleckner, 1998 The leptotene-zygotene transition of meiosis. Annu. Rev. Genet. **32:** 619–697.

Zimmer, E. A., E. R. Juppe and V. Walbot, 1988 Ribosomal gene structure variation and inheritance in maize and its ancestors. Genetics **120:** 1125–1136.

Communicating editor: J. A. Birchler